RESEARCH ACTIVITIES IX
Laser Research Center for Molecular Science

IX-A Developments and Researches of New Laser Materials

Although development of lasers is remarkable, there are no lasers which lase in ultraviolet and far infrared regions. However, it is expected that these kinds of lasers break out a great revolution in not only the molecular science but also in the industrial world.

In this project we research characters of new materials for ultraviolet and far infrared lasers, and develop new lasers by using these laser materials.

IX-A-1 Terahertz Radiation Mechanism from Femtosecond-Laser-Irradiated InAs (100) Surface

TAKAHASHI, Hiroshi[1]; QUEMA, Alex; GOTO, Masahiro; ONO, Shingo; SARUKURA, Nobuhiko
([1]GUAS)

[*Jpn. J. Appl. Phys.* **42**, L1259 (2003)]

Terahertz (THz) radiation mechanism from femtosecond-laser-irradiated InAs surface is investigated by measuring the excitation-fluence dependence of THz-radiation power. It is found that the THz-radiation is mainly generated by the surge-current, which originates from the different diffusion velocities between photo-excited electrons and holes. Furthermore, it is also found that the excitation fluence dependence of THz-radiation is categorized into two regions depending on the excitation fluence. At low excitation fluence, a quadratic-dependent enhancement of the THz-radiation power is observed with increasing excitation fluence. In contrast, at high excitation fluence, the enhancement factor is gradually reduced, and the radiation power becomes proportional to a logarithm function of the excitation fluence. These results are explained by considering the photo-Dember field as the THz-radiation source.

IX-A-2 Broadband Terahertz Radiation Emitter Using Femtosecond-Laser-Irradiated *n*-Type InAs under Magnetic Field

TAKAHASHI, Hiroshi[1]; HASSELBECK, Michael[2]; QUEMA, Alex; GOTO, Masahiro; ONO, Shingo; SARUKURA, Nobuhiko
([1]GUAS; [2]Univ. New Mexico)

[*Jpn. J. Appl. Phys.* **43**, L221 (2004)]

We present the generation of broadband terahertz (THz) radiation using *n*-type InAs irradiated by ultrafast laser pulses. It is found that the high-frequency component of the THz-radiation spectrum originates from the hybrid modes of the plasmons and the longitudinal optical (LO) phonons, whose peak frequency shifts toward higher frequency with increasing doping density. For *n*-type InAs with a doping density of 3.1×10^{17} cm^{-3}, the high-frequency components of THz-radiation spectrum are observed at around 5.5 and 9 THz. Furthermore, the enhancement of THz-radiation power from these hybrid modes is achieved by applying an external magnetic field.

IX-A-3 Teflon Photonic Crystal Fiber as Terahertz Waveguide

GOTO, Masahiro; QUEMA, Alex; TAKAHASHI, Hiroshi; ONO, Shingo; SARUKURA, Nobuhiko

[*Jpn. J. Appl. Phys.* **43**, L317 (2004)]

We demonstrate the construction of reasonably long and non-polarization changing photonic fiber waveguide using Teflon which is a readily available and highly flexible material. Due to its relatively low loss coefficient, the possibility of preparing longer photonic fiber waveguide,which has the potential of guiding intense THz radiation, can be easily attained.

IX-A-4 Growth and Charge Transfer Luminescence of Yb^{3+}-Doped $YAlO_3$ Single Crystals

SHIM, Jan Bo[1]; YOSHIKAWA, Akira[1]; FUKUDA, Tsuguo[1]; PEJCHAL, J.[2]; NIKL, M.[2]; SARUKURA, Nobuhiko; YOON, D. H.[3]
([1]Tohoku Univ.; [2]Inst. Phys. ASCR; [3]Sungkyunkwan Univ.)

[*J. Appl. Phys.* **95**, 3063 (2004)]

Yb^{3+}-doped $YAlO_3$ single crystals have been grown by the Czochralski method with a radio-frequency heating system. Starting melt compositions of $Y_{1-x}Yb_xAlO_3$ were varied with x = 0.02, 0.1, 0.2, 0.3, and 0.45. The best Yb^{3+}-doped $YAlO_3$ single crystals were obtained for a growth rate of 1.0 mm/h. The grown crystals were transparent and almost colorless. To investigate the homogeneity, the effective segregation coefficient of the Yb ion was estimated. The absorption, photoluminescence, and luminescence decay kinetics of Yb^{3+}-doped $YAlO_3$ were investigated for the temperature range 4–300 K. Very fast charge transfer luminescence of Yb^{3+} from the near ultraviolet to visible spectral range and the high density of the Yb-rich $YAlO_3$ makes this material a promising candidate for fast scintillators.

IX-A-5 Terahertz Radiation from InAs with Various Surface Orientations under Magnetic Field Irradiated with Femtosecond Optical Pulses at Different Wavelengths

TAKAHASHI, Hiroshi[1]; SAKAI, Masahiro; QUEMA, Alex; ONO, Shingo; SARUKURA, Nobuhiko; NISHIJIMA, Gen[2]; WATANABE, Kazuo[2]
([1]GUAS; [2]Tohoku Univ.)

[*J. Appl. Phys.* **95**, 4545 (2004)]

We present the magnetic-field dependence of terahertz (THz)-radiation power from femtosecond-laser-irradiated InAs with various surface orientations. Under 800 nm optical excitation, the magnetic field that provides the maximum THz-radiation power is found to be affected by the surface orientation, and InAs(111) exhibits it at lower magnetic fields than that of the other surfaces. In contrast, under 1560 nm excitation, the dependence on the surface orientation almost disappeared, and saturation is observed at a much smaller magnetic field than that in the 800 nm excitation case. Additionally, from the results of magnetic-field dependence up to 14 T, the shift of the peak in the THz-radiation spectrum toward lower frequency is confirmed, depending on the magnetic field applied, which is possibly induced by the emergence of a magneto-plasma effect.

IX-A-6 Optical, Infrared and EPR Spectroscopy of CaF_2:Ce^{3+} Crystals Co-Doped with Li^+ or Na^+

YAMAGA, Mitsuo[1]; YABASHI, Satoshi[1]; MASUI, Yuki[1]; TAKAHASHI, Hiroshi; SAKAI, Masahiro; SARUKURA, Nobuhiko; WELLS, J. -P. R.[2]; JONES, G. D.[3]
([1]Gifu Univ.; [2]Univ. Sheffield; [3]Univ. Canterbary)

[*J. Lumin.* **108**, 307 (2004)]

Interconfigurational 4f ↔ 5d VUV absorption and luminescence, intra-4f[1] IR absorption and X-band EPR measurements have been carried out on CaF_2:Ce^{3+} crystals co-doped with Na^+ and Li^+ ions. For both Li^+ and Na^+ co-doping, cubic, new tetragonal and rhombic-symmetry centres are observed. Cubic centres, which are readily observable by their infrared transitions, could not be identified and remain elusive in the EPR spectra.

IX-A-7 Effect of Ultrafast Optical Pulses with Different Pulse Duration on the Terahertz Radiation Spectrum of *n*-Type InAs

TAKAHASHI, Hiroshi[1]; HASSELBECK, Michael[2]; QUEMA, Alex; GOTO, Masahiro; ONO, Shingo; SARUKURA, Nobuhiko
([1]GUAS; [2]Univ. New Mexico)

[*Jpn. J. Appl. Phys.* **43**, L746 (2004)]

Terahertz (THz) radiation from *n*-type InAs irradiated by ultrafast laser pulses is investigated under the existence of the magnetic field. It is found that the high-frequency component of the THz-radiation spectrum originates from the hybrid modes of the plasmons and the longitudinal optical (LO) phonons, and its intensity can be drastically enhanced by using the laser pulses with duration shorter than the oscillation period of the hybrid modes. Additionally, it is also found that the ratio of THz-radiation power from these two modes can be controlled by adjusting the pulse duration and the magnetic field strength.

IX-A-8 Physical Origin of Magnetically Induced Periodic Structure Observed in Terahertz Radiation Spectrum Emitted from InAs

TAKAHASHI, Hiroshi[1]; QUEMA, Alex; GOTO, Masahiro; ONO, Shingo; SARUKURA, Nobuhiko; NISHIJIMA, Gen[2]; WATANABE, Kazuo[2]
([1]GUAS; [2]Tohoku Univ.)

[*Jpn. J. Appl. Phys.* **43**, L1017 (2004)]

Terahertz (THz) radiation from femtosecond-laser-irradiated InAs(100) surface is investigated. It is found that THz-radiation spectrum exhibits two inter-related phenomena in a strong magnetic field under the Voigt configuration. The peak shift of THz-radiation spectrum toward lower frequency is observed with increasing magnetic field. Additionally, THz-radiation spectrum is found to posses a periodic structure owing to the interference of THz-radiation pulses from the front and back surfaces of the InAs substrate. The physical origin of the latter phenomenon is discussed by considering the magneto-plasma effect, which affects both real and imaginary parts of refractive index for THz-radiation propagating in a direction perpendicular to the magnetic field.

IX-A-9 Design Proposal of Light Emitting Diode in Vacuum Ultraviolet Based on Perovskite-Like Fluoride Crystals

OUENZERFI, El Riadh[1]; ONO, Shingo; QUEMA, Alex; GOTO, Masahiro; SARUKURA, Nobuhiko; NISHIMATSU, Takeshi[1]; TERAKUBO, Noriaki[1]; MIZUSEKI, Hiroshi[1]; KAWAZOE, Yoshiyuki[1]; YOSHIKAWA, Akira[1]; FUKUDA, Tsuguo[1]
([1]Tohoku Univ.)

[*Jpn. J. Appl. Phys.* **43**, L1140 (2004)]

The variation of band gap energy, band structure and lattice constant of mixed $LiBaF_3$, $LiCaF_3$ and $LiSrF_3$ perovskites is studied. The band structure and transition type of these fluorides is predicted by *ab initio* band calculation based on the local density approximation. The design principle of vacuum ultraviolet light emitting diode is proposed. The lattice-matched double-hetero structure of different perovskite-like fluorides is found to be sufficiently feasible to fabricate with direct-band-gap compounds $LiBa_xCa_ySr_{(1-x-y)}F_3$ on $LiSrF_3$.

IX-B Development and Research of Advanced Tunable Solid State Lasers

Diode-pumped solid-state lasers can provide excellent spatial mode quality and narrow linewidths. The high spectral power brightness of these lasers has allowed high efficiency frequency extension by nonlinear frequency conversion. Moreover, the availability of new and improved nonlinear optical crystals makes these techniques more practical. Additionally, quasi phase matching (QPM) is a new technique instead of conventional birefringent phase matching for compensating phase velocity dispersion in frequency conversion. These kinds of advanced tunable solid-state light sources, so to speak "Chroma Chip Lasers," will assist the research of molecular science.

In this projects we are developing Chroma Chip Lasers based on diode-pumped-microchip-solid-sate lasers and advanced nonlinear frequency conversion technique.

IX-B-1 Saturation Factors of Pump Absorption in Solid-State Lasers

SATO, Yoichi; TAIRA, Takunori

[*IEEE J. Quantum Electron.* **40**, 270–280 (2004)]

The precise formulation of the absorption coefficient is investigated, where the saturation factors of absorption for solid-state lasers are defined as depending on the pumping scheme. We also investigated theoretical and experimental evaluations of the pump saturation effect in Nd:YVO_4 as an example, and proved the accuracy of this model describing the saturation effect (Figure 1), and the clipping of this effect by laser oscillation (Figure 2). This paper points out the following: even in the case of 1 μm oscillation in neodymium lasers, the selection of pump wavelength results in not only the different absorption cross sections, but also the different characteristics in the saturation of the pump absorption. This influence is especially important in the laser media with a large cross section, such as Nd:YVO_4. For example, in the direct pumping into the emitting levels $^4F_{3/2}$, the electrons in the laser upper level also connect to the stimulated emission to the ground state, which should not be observed in the conventional pumping into $^4F_{5/2}$ because of little distribution of the electrons in the $^4F_{5/2}$.

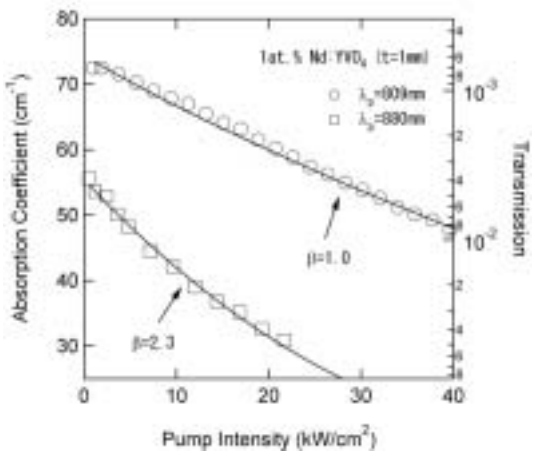

Figure 1. Absorption coefficient of 1 at.% Nd:YVO_4 in π-polarization as a function of pumping intensity.

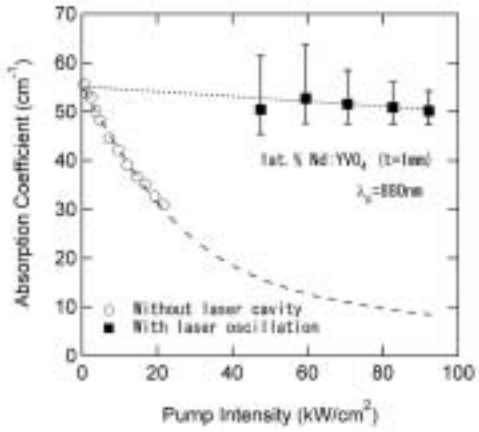

Figure 2. Absorption coefficient of 1 at.% Nd:YVO_4 in π-polarization under lasing condition.

IX-B-2 Spectroscopic Properties and Laser Operation of Nd:$Y_3ScAl_4O_{12}$ Polycrystalline Gain Media, Solid-Solution of Nd:$Y_3Al_5O_{12}$ and Nd:$Y_3Sc_2Al_3O_{12}$ Ceramics

SATO, Yoichi; SAIKAWA, Jiro; SHOJI, Ichiro; TAIRA, Takunori; IKESUE, Akio

[*J. Ceram. Soc. Jpn.* **112**, S313–S316 (2004)]

Transparent Nd^{3+}-doped $Y_3ScAl_4O_{12}$ (Nd:$Y_3ScAl_4O_{12}$) ceramics with up to 5.0-at.% Nd^{3+}-concentration (C_{Nd}) were fabricated by a solid-state reaction method using commercial 4N powders. Spectroscopic properties of this media, such as absorption and emission spectra, the fluorescence lifetime, and the influence of increasing C_{Nd} on these characteristics are discussed. It is shown that high absorption efficiency of the pump radiation that is necessary for efficient operation of a Nd:$Y_3ScAl_4O_{12}$ microchip laser can be obtained by increasing C_{Nd}. One-micron laser operation with 113-mW output power (7.7% optical-to-optical overall efficiency) and 9.6% slope efficiency was demonstrated from a 1.0-mm thick, 5.0-at.% Nd:$Y_3ScAl_4O_{12}$ uncoated sample under 808-nm pumping by a Ti:Sapphire laser (Figure 1). Further works are directed toward optimization of the fabricating process in order to reduce the optical losses that are found to increase with increasing C_{Nd}.

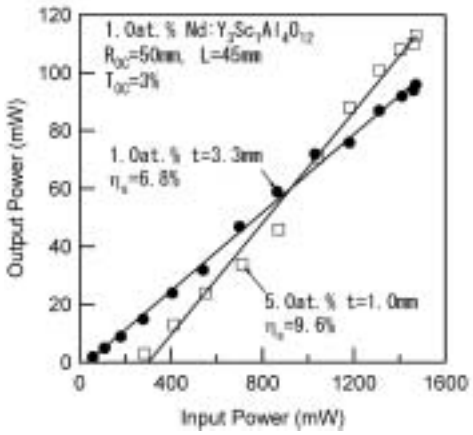

Figure 1. Output power versus pump power for the Nd:$Y_3Sc Al_4O_{12}$ ceramics with 1.0 and 5.0-at.% Nd under 808-nm Ti:Sapphire pumping.

IX-B-3 High Energy Optical Parametric Oscillation Using 3-mm-Thick Periodically Poled MgO:$LiNbO_3$

ISHIZUKI, Hideki; SHOJI, Ichiro; TAIRA, Takunori

[*Conf. Lasers Electro-Optics* CTuA3 (2004)]

We presented high energy optical parametric oscillation (OPO) using 3-mm-thcik periodically poled MgO:LN (PPMgLN) device. Multipulses of ~10 kV were applied to the crystal at elevated temperature of ~100 °C to fabricate the PPMgLN device.

For OPO experiments, a Q-switched Nd:YAG laser (Spectra-Physics, LAB-170-30) was used as a pump source. The repetition rate was 30 Hz with the pulse width of 15 ns. The cavity length of single resonant OPO was fixed to 35 mm. The $1/e^2$-diameter of pump beam was set to 2.2 mm. Figure 1 shows the dependence of OPO output energy on input pump energy. The pump threshold was ~3 mJ, and the slope efficiency was 51% for total output (signal of 1.82 μm, idler of 2.56 μm) and 28% for the signal wave only. The maximum total output energy of 22 mJ at the pump energy of 46 mJ was obtained without photorefractive damages. This is the highest energy obtained from QPM-OPO operation using a PPMgLN device even at room temperature. The large-aperture PPMgLN devices would enable us to realize high-energy wavelength conversion, short pulse amplification, and pulse compression.

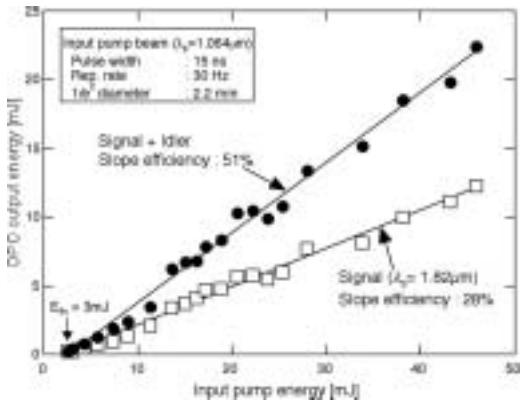

Figure 1. OPO output energy *vs.* input pump energy. Pump pulse width : 15 ns, Pump rep. rate : 30 Hz, Pump $1/e^2$-diameter : 2.2 mm.

IX-B-4 Basic Enhancement of the Overall Optical Efficiency of Intracavity Frequency-Doubling Devices for the One-Micron Continuous-Wave Nd:$Y_3Al_5O_{12}$ Laser Emission

LUPEI, Voicu[1]; PAVEL, Nicolaie[2]; TAIRA, Takunori
([1]IAP-NILPRP, Romania; [2]IMS and IAP-NILPRP, Romania)

[*Appl. Phys. Lett.* **83**, 3653 (2003)]

Frequency-doubling of the efficient one-micron $^4F_{3/2} \rightarrow {}^4I_{11/2}$ Nd^{3+} lasers is currently the most used method to obtain light into the green region. If the intracavity frequency-doubling method is considered, the laser active material and a nonlinear crystal designed for phase matching conditions are placed in a laser resonator that confines the beam at the fundamental frequency ω inside the resonator, passes it through the doubling crystal and out-couples the frequency-doubled 2ω beam. The second-harmonic (SH) power $P_{2\omega}$ is determined by the intracavity emission intensity of the active material $I_{\omega,\mathrm{int}}$ and by the characteristics of the doubling crystal

$$P_{2\omega} \sim I_{\omega,\mathrm{int}}^2 \cdot d_{eff}^2 \ell^2 / (n_1^2 n_2) \qquad (1)$$

where d_{eff} is the effective nonlinear coefficient along the phase matching direction, l is the length of the nonlinear crystal and n_1 and n_2 are the refractive indices at the fundamental and SH wavelengths, respectively. The overall optical-to-optical efficiency of such a laser, i.e. the output power $P_{2\omega}$ obtained for a given pump power $P^{(j)}$, where $j \equiv i$ denotes the pump power incident on the laser material and $j \equiv ab$ denotes the absorbed power, can be optimized acting on these factors. In this work we discuss the possibility of basic enhancement of the overall optical-to-optical efficiency of intracavity frequency-doubling devices for the one-micron continuous-wave Nd lasers by direct pumping into the emitting level and by using concentrated laser materials.

The continuous wave (CW) Nd lasers are usually pumped using the strong absorption Nd^{3+} lines to energy levels placed above the emitting level $^4F_{3/2}$ and the absorbed excitation relaxes to the emitting level through electron-phonon interactions. Thus, the upper

quantum defect between the pump level and the emitting level reduces the performances of the laser emission and contributes to the generation of heat. The upper quantum defect can be eliminated by pumping directly into the emitting level $^4F_{3/2}$: this modality of pumping was suggested in the first work on semiconductor diode excitation of Nd^{3+} emission[1] and it was used in the first diode laser pumped Nd:YAG both in transverse and end-pumped configurations.[2),3)] However, owing to the weak absorption into the level $^4F_{3/2}$ of Nd^{3+} in YAG, this was soon replaced by diode laser pumping at 808 nm into the strongly absorbing level $^4F_{5/2}$. The direct pumping of CW Nd lasers into the emitting level was reconsidered recently for Nd:YAG crystals and ceramics[4),5)] as well as for other laser materials, such as Nd:YVO_4[4),6)] or Nd:$GdCa_4O(BO_3)_3$.[7)]

A problem of concern in using the direct pumping into the emitting level is the low absorption η_a in some of the important laser materials, including Nd:YAG, for concentrations C_{Nd} around 1-at.% Nd that are traditionally used for construction of lasers. This could be overcome by using more concentrated materials. By estimating the quantum efficiency η_{qe} using the energy transfer data at low inversion, specific to the CW Nd:YAG lasers, it was shown that the product $\eta_a\eta_{qe}$ increases with C_{Nd} up to a critical value then decreases again.[5)] The range of CNd for which this product is larger than for 1-at.% Nd could be quite wide: up to 8.0-at.% for Nd:YAG and up to 3.0-at.% for Nd:YVO_4. Thus, working at the upper C_{Nd} limit would benefit both from a low threshold and from increased slope efficiency.

According to Eq. (1), the enhancement of the laser emission parameters at the frequency ω by direct pumping will be accentuated in the frequency-doubling device, resulting in a lower threshold for the SH emission and in a stronger dependence on the absorbed pump power. These concepts are investigated in this work by using 1.0-at.% and 2.4-at.% Nd:YAG crystals.

The frequency doubling is investigated with a V-type folded laser resonator (Figure 1). The 3-mm long Nd:YAG crystals were coated as anti-reflection for 1064 nm and high transmission for 808 and 885 nm. A Ti:Sapphire laser whose radiation was focused into the crystals in a spot of 50-μm diameter was used for pumping. The M1 to M2 resonator arm is 70-mm long and contains also a Brewster glass plate (BP) to polarize the beam. The length of the M2 to M3 frequency-doubling arm was 55 mm and houses a 10-mm long LBO nonlinear crystal designed for type I critical phase matching condition (θ = 90°, ϕ = 11.4°) at 25 °C.

The 532-nm output power for the 1.0-at.% Nd:YAG crystal is shown in Figure 2. The threshold of green radiation is greatly reduced at 885 compared to 808-nm pumping (26 and respectively 50 mW), while the dependence on the absorbed power is enhanced. Moreover, the emission under 808-nm pumping shows signs of saturation induced by thermal effects in Nd:YAG for green emission larger than ~14 mW. The 532-nm emission under 885-nm pumping does not show such behavior even at the 20 mW obtained for the available absorbed power. As indicated by Figure 3a, the use of a more concentrated (2.4-at.% Nd) active crystal improves the 885-nm pump absorption efficiency, but increases the emission threshold in absorbed power, without changing the slope efficiency. However, the SH power obtained with this sample for a given incident power is larger (Figure 3b). Further improvement could be obtained with a longer active laser crystal and/or a higher C_{Nd}.

In conclusion this work demonstrates the advantages of using direct pumping into the emitting level and of more concentrated laser materials in intracavity frequency-doubling devices based on the 1064-nm CW laser emission of Nd:YAG. The improvement of emission parameters is accompanied by a drastically reduction of generation of heat that could enable scaling to higher emission powers. This approach could be particularly important for laser materials with higher absorption cross-section for the direct pumping.

References

1) R. Newman, *J. Appl. Phys.* **34**, 437 (1963).
2) M. Ross, *Proc. IEEE* **56**, 196 (1968).
3) L. J. Rosenkrantz, *J. Appl. Phys.* **34**, 4603 (1972).
4) R. Lavi, S. Jackel, Y. Tzuk, M. Winik, E. Lebiush, M. Katz and I. Paiss, *Appl. Opt.* **38**, 7382 (1999).
5) V. Lupei, N. Pavel and T. Taira, *IEEE J. Quantum Electron.* **38**, 240 (2002).
6) V. Lupei, N. Pavel and T. Taira, *Opt. Commun.* **201**, 431 (2002).
7) V. Lupei, D. Vivien and G. Aka, *Appl. Phys. Lett.* **81**, 811 (2002).

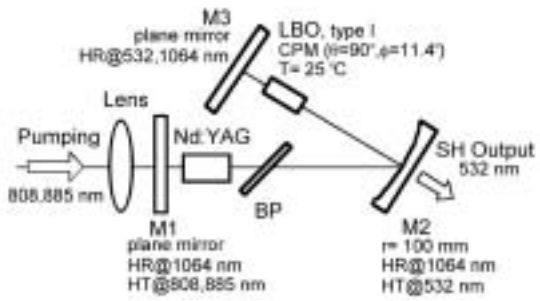

Figure 1. Schematic of the V-type resonator used in intracavity frequency-doubling experiments.

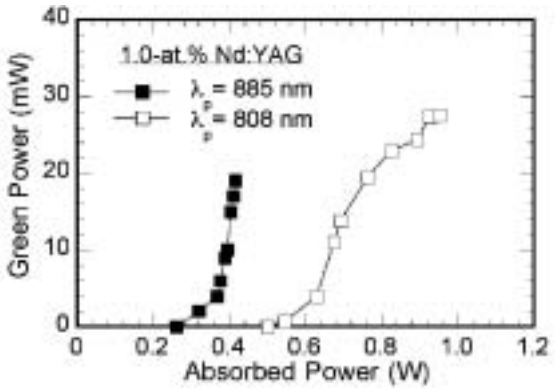

Figure 2. Green power *vs.* absorbed power for the 1.0-at.% Nd:YAG crystal under 808 and 885-nm pumping.

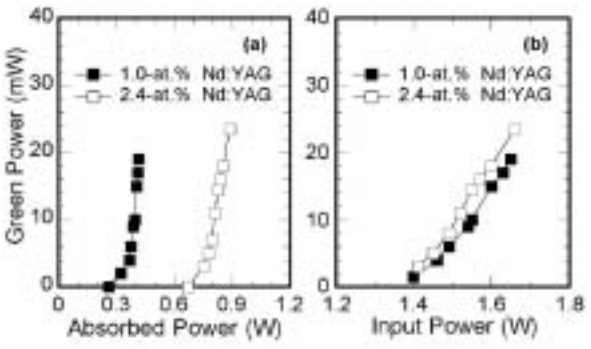

Figure 3. Green power for the 1.0 and 2.4-at.% Nd:YAG crystals under 885-nm pumping function of (a) absorbed, and (b) input power.

IX-B-5 High-Power Blue Generation from a Periodically Poled MgO:$LiNbO_3$ Ridge-Type Waveguide by Frequency Doubling of a Diode End-Pumped Nd:$Y_3Al_5O_{12}$ Laser

IWAI, Makato[1]; YOSHINO, Takeshi[1]; YAMAGUCHI, Shoichiro[1]; IMAEDA, Minoru[1]; PAVEL, Nicolaie[2]; SHOJI, Ichiro; TAIRA, Takunori

([1]NGK, Nagoya; [2]IMS and IAP-NILPRP, Romania)

[*Appl. Phys. Lett.* **83**, 3659 (2003)]

Continuous-wave (CW) blue laser radiation is of interest for various applications, such us display technologies, obtaining of high-density optical disk systems, high-resolution printing, or biological application. In order to obtain the blue light at 473 nm the second-harmonic generation (SHG) of the $^4F_{3/2} \rightarrow {}^4I_{9/2}$ transition at 946 nm of Nd^{3+}:$Y_3Al_5O_{12}$ (Nd:YAG) can be used. An attractive method to realize a compact blue-light source is SHG by quasi-phase matching (QPM) interaction: $LiNbO_3$ (LN), $LiTaO_3$ and $KTiOPO_4$ are in present widely known and used for fabricating of QPM devices. CW blue light at 473 nm of 81 mW was generated for a fundamental power of 1.13 W in a 15-mm-long periodically poled (PP) $LiNbO_3$ that operated at an elevated temperature of 140 °C.[1)] When using a PP $KTiOPO_4$ pumped at room temperature by a 946-nm Nd:YAG laser maximum blue power of 76 mW was obtained for 2.27 W of fundamental power.[2)]

Due to its high conversion efficiency, a waveguide-type QPM SHG device is a very promising solution for a compact blue-light source. The key points for obtaining efficient and high-power SHG waveguide devices include strong confinement of the fundamental light into the waveguide, good overlap of fundamental and second-harmonic modes, prevention of nonlinear properties degradation, maintaining of a high optical-damage resistance, particularly in the shorter wavelength region. MgO:$LiNbO_3$ (MgO:LN) was demonstrated to be a good nonlinear material for blue generation: compared with non-doped LN, it presents higher resistance to photorefractive damage, decreased coercive field and a large nonlinear coefficient $d_{33} \sim 25$ (±2.5) pm/V.[3),4)] CW blue power of 17.3 mW at 426 nm was demonstrated from a AlGaAs laser diode with 55-mW output power by using a MgO:LN proton-exchanged waveguide.[5)] However, these waveguides has some limitations, such as mode field mismatching caused by dispersion and refractive index profiles, a trade-off between index change and nonlinearity[6)] that degrades to about 90% of the original d_{33} value even after annealing.

In order to overcome these problems a fabrication process for realizing high efficiency and high power SHG waveguide devices by bonding and ultra-precision machining techniques was introduced by our group: thus, a ridge-type waveguide QPM-SHG MgO:LN device that preserves the original performances of the nonlinear crystal can be obtained. This research reports on our efforts toward scaling blue light obtained by frequency-doubling from a PP MgO:LN ridge-type waveguide using a diode end-pumped Nd:YAG laser operating at 946 nm as a fundamental source.

Based on the relation between the wavelength tuning of SHG and the periodicity of domain-inverted regions, a ridge-type MgO:LN waveguide of 4.6 μm periodicity was fabricated by ultra-precision machining to generate blue light at 473 nm. Figure 1 shows the procedure of fabrication. First, the periodically domain-inverted regions were formed on a MgO:LN substrate (3°-off X-cut) by the 2D high-voltage application technique (Figure 1a). Then a resin adhesive was used to glue the obtained comb-electrode-formed surface to a LN substrate (Figure 1b). In the next step (Figure 1c) the MgO:LN substrate was thinned by flat-grinding and surface finishing: thus, a 4 μm-thick planar waveguide was realized. In the final step (Figure 1d), the ridge-shaped structure was processed by machining to form a ridge-type waveguide.

A sketch of the experimental set-up is presented in Figure 2. The fundamental 946-nm radiation for frequency doubling was provided by a home-made Nd:YAG laser. For an absorbed pump power at 809 nm of 4.2 W the polarized output was 1.1 W in a Gaussian distribution ($M^2 = 1.05$); the slope efficiency was 38%. Three periodically poled MgO:LN ridge-type waveguides, each of 1.4 mm-width, were prepared. First one has 8.5-mm length and both the input and output surfaces were cut at an angle $\alpha = 10°$ and AR coated at 946 nm by SiO_2 monolayer. The second one of 6-mm length has the input and output surfaces cut at $\alpha = 10°$, while the third one has 12-mm length and only the input surface cut at $\alpha = 6°$; these two samples have no coating at 946 nm. No coating was provided at 473 nm for all the waveguides. The MgO:LN ridge-type waveguide was placed on an aluminum plate whose temperature was controlled within 0.1 °C accuracy.

The 473-nm power as a function of the 946-nm power coupled into the waveguide is presented in Figure 3. The maximum blue power of 189 mW was obtained for the 8.5-mm-long MgO:LN waveguide with a conversion efficiency of 49%. If the Fresnel loss on the waveguide output surface is considered, the maximum internal blue-light power is 222 mW, corresponding to a conversion efficiency of 58%. As the fundamental power before the waveguide was 670 mW the overall conversion efficiency is 28%; improving the 946 nm radiation coupling efficiency into the waveguide could increase the device overall efficiency. The maximum blue power for the 6-mm-long MgO:LN waveguide was 155 mW with 42% conversion efficiency (182-mW blue

internal power with 49% conversion efficiency), while 147 mW with a conversion efficiency of 48% (173-mW blue internal power with 56% conversion efficiency) were obtained for the 12-mm-long MgO:LN waveguide. The highest conversion efficiency of 63% (internal conversion efficiency of 74%) was obtained for a blue power of 99 mW from the longest waveguide used in experiments. During an hour measurement, the peak-to-peak fluctuations for the 946-nm maximum power were ±1.3%, while the blue power fluctuations were ±4.0%. The phase matching temperature was 36.3 °C and the measured acceptance bandwidth ΔT was 2.3 °C, in very good agreement with the predicted theoretical value of 2.35 °C.

In conclusion, CW blue-light generation from a periodically poled MgO:$LiNbO_3$ waveguide by frequency-doubling of a diode end-pumped Nd:YAG laser operating at 946 nm is reported. The maximum output power at 473 nm was 189 mW with 49% conversion efficiency (222 mW internal power with 58% conversion efficiency), indicating the potential for high-power SHG of the ridge-type waveguide fabricated by ultra-precision machining.

References

1) G. W. Ross, M. Pollnau, P. G. R. Smith, W. A. Clarkson, P. E. Britton and D. C. Hanna, *Opt. Lett.* **23**, 171 (1998).
2) S. Spiekermann, H. Karlsson and F. Laurell, *Appl. Opt.* **40**, 1979 (2001).
3) I. Shoji, T. Kondo, A. Kitamoto, M. Shirane and R. Ito, *J. Opt. Soc. Am. B* **14**, 2268 (1997).
4) A. Kuroda, S. Kurimura and Y. Uesu, *Appl. Phys. Lett.* **69**, 1565 (1999).
5) T. Sugita, K. Mizuuchi, Y. Kitaoka and K. Yamamoto, *Opt. Lett.* **24**, 1590 (1999).
6) K. Mizuuchi, H. Ohta, K. Yamamoto and M. Kato, *Opt. Lett.* **22**, 1217 (1997).

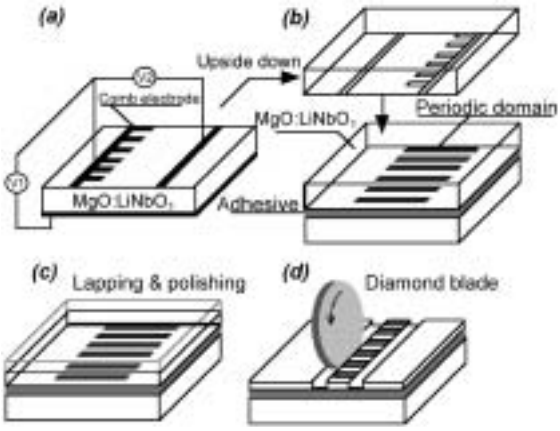

Figure 1. Fabrication steps of a periodically poled MgO:LN ridge-type waveguide by ultra-precision machining: (a) obtaining of the domain-inverted regions, (b) adhesion with a LN substrate, (c) flat grinding and polishing, and (d) ultra-precision grinding.

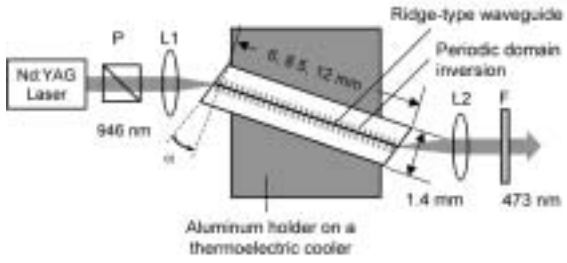

Figure 2. Schematic diagram of the experimental set-up. P: polarizer; L1: focusing lens; L2: collimating lens; F: 946-nm cut filter.

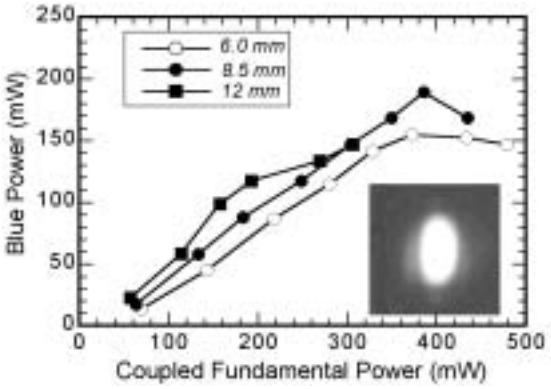

Figure 3. Output power at 473 nm versus the 946-nm power coupled into the waveguide. The inset shows a typical blue light far-field distribution.

IX-B-6 High-Power Continuous Wave Green Generation by Single-Pass Frequency Doubling of a Nd:$GdVO_4$ Laser in a Periodically Poled MgO:$LiNbO_3$ Operating at Room Temperature

MIZUUCHI, Kiminori[1]; MORIKAWA, Akihiro; SUGITA, Tomoya[1]; YAMAMOTO, Kazuhisa[1]; PAVEL, Nicolaie[2]; SHOJI, Ichiro; TAIRA, Takunori

([1]Matsushita Co., Ltd., Osaka; [2]IMS and IAP-NILPRP, Romania)

[*Jpn. J. Appl. Phys.* **42**, L1296 (2003)]

Due to its high effective nonlinear coefficient and the possibility of obtaining non-critical phase matching in single-pass continuous wave (CW) pumping scheme, the periodically poled $LiNbO_3$ (PPLN) crystal continues to attract a great interest as a QPM device for generation in blue, green, or violet ranges. Employing a 50-mm-long first-order PPLN sample, CW powers of 2.7-W green[1)] and 60-mW blue[2)] were demonstrated, respectively. It is known, however, that PPLN has significant problems for visible light radiation, such as green-induced infrared absorption and optical damage. Although phase matching at high temperature close of 200 °C was used,[2)] power instabilities and thermal lens effects could not be completely suppressed. Thus, to date, room temperature CW operation close or in excess of 1 W level was not obtained from a single-pass pumped PPLN crystal.

In order to overcome these problems, it was recently proposed[3)] to utilize periodically poled MgO:$LiNbO_3$

(PPMgLN). Due to its larger nonlinear susceptibilities, higher resistance against photorefractive damage and shorter wavelength transparency compared with PPLN, PPMgLN is a very attractive material for generation of visible light through SHG by QPM process. Moreover, because of its low coercive field,[4] it was demonstrated that PPMgLN could be fairly easily fabricated by means of electric field poling. Recently, a novel high-voltage multi-pulse poling technique that suppress the penetration of poled region and produces uniform PPMgLN with domain period (Λ) as short as 1.4 μm was developed by our group.[5] This letter reports CW SHG at room temperature in a first-order PPMgLN with Λ = 6.95 mm that was fabricated by this technique.

In order to improve the domain pattern quality for short periodic structure a special attention was paid to understand the domain formation processes in a z-cut MgLN crystal. A large resistance reduction was found in a 0.5-mm-thick z-cut MgLN during a conventional electric-field-poling process. Large leakage current was observed in the electric circuit after poling process, which was explained by the resistance reduction in the poled region from 6×10^{11} to 7×10^{5} Ω·mm. This large resistance reduction may cause irregular side growth and non-uniformity of polarization inversion that, in turn, interrupts the fabrication of short-periodic structures. Such local penetrations under the electrode may shorten the surface and bottom electrodes and cause large leakage current between electrodes, which degrade uniformity of electric field. Then, in order to realize uniform PPMgLN structure over large areas, local penetration of polarization-inverted regions must be suppressed: a thick crystal and the multi-pulse application method[6] are used to overcome this last problem. The penetration of polarization inversion to the bottom of the crystal could be suppressed by employing thick samples. Shortening the growth time by using short width pulse would control the forward growth, while multiple pulses should supply enough charge for realizing a relatively deep polarization-inverted structure. Figure 1 shows the cross-sectional of the PPMgLN with Λ = 6.95 mm for various depths: the structure presents 50% duty cycle from the +Z surface to a depth of ~300 μm and uniform periodicity was maintained from the surface to ~800-μm depth.

The 1063-nm radiation for frequency doubling was provided by a home-made diode end-pumped Nd:$GdVO_4$ laser that delivers CW 6.8 W output power (M^2 factor of 1.16) for an 808-nm pump power measured at the fiber end of 15.1 W; the slope efficiency was 57%. The output beam depolarization ratio was 1.2% and the power fluctuation during few hours of operation was ±1.1%. For SHG experiments a 10-mm length PPMgLN was used: the PPMgLN end-faces were optically polished and anti-reflection (AR) coated by SiO_2 monolayer for the 1063-nm fundamental wavelength; no coating was provided at 531 nm. The PPMgLN was placed on an aluminum plate whose temperature was controlled within 0.1 °C accuracy with a thermoelectric cooler. The 1063-nm radiation was focused into PPMgLN to a spot size of 17-μm radius.

Figure 2 shows the 531-nm green power after PPMgLN versus the 1063-nm fundamental power measured after the focusing lens. The maximum green power of 0.89 W was obtained for an infrared incident power of 6.23 W, resulting a conversion efficiency of 14.3%. If the Fresnel loss (determined as ~14%) on the output surface is considered the maximum internal green-light power results as 1.03 W, corresponding to a conversion efficiency of 16.5%. The effective nonlinear coefficient was determined as 14 pm/V and the normalized conversion efficiency including the Fresnel loss by reflection was 2.7%/W. Figure 2 shows by continuous line the theoretical modeling using a quadratic relation with this value: a good agreement with the experimental results is observed. The phase matching temperature was 29.5 °C, stable within ±0.3 °C on the entire pumping range.

In conclusion, irregular side growth of polarization inversion was suppressed in a 2-mm thick PPMgLN by using a multi-pulse application poling method. Uniform periodicity and 50% duty cycle with a 6.95-μm domain period was fabricated on 10-mm length of interaction. This structure was used to obtain perfect first-order QPM in the bulk PPMgLN at 1063 nm wavelength: CW 531-nm green light of 0.89 W with 14.2% power conversion efficiency was obtained (internal power of 1.03 W and 16.5% conversion efficiency) in a single-pass pumping with a Nd:$GdVO_4$ laser.

References

1) G. D.Miller, R. G. Batchko, W. M. Tulloch, D. R. Weise, M. M. Fejer and R. L. Byer, *Opt. Lett.* **22**, 1834 (1997).
2) R. G. Batchko, M. M. Fejer, R. L. Byer, D. Woll, R. Wallenstein, V. Y. Shur and L. Erman, *Opt. Lett.* **24**, 1293, (1999).
3) K. Mizuuchi, K. Yamamoto and M. Kato, *Electron. Lett.* **32**, 2091 (1996).
4) A. Kuroda, S. Kurimura and Y. Uesu, *Appl. Phys. Lett.* **69**, 1565 (1996).
5) K. Mizuuchi, A. Morikawa, T. Sugita and K. Yamamoto, *Jpn. J. Appl. Phys.* **42**, L90 (2003).
6) T. Sugita, K. Mizuuchi, Y. Kitaoka and K. Yamamoto, *Jpn. J. Appl. Phys.* **40**, 3B-222 (2001).

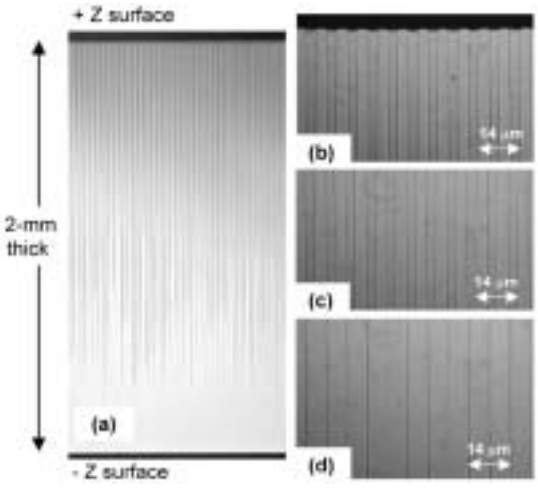

Figure 1. Cross-sectional view (Y face) of first-order PPMgLN with Λ = 6.95 μm: (a) general view, (b) near the surface, (c) at the depth of 300 μm, and (d) at 1-mm depth.

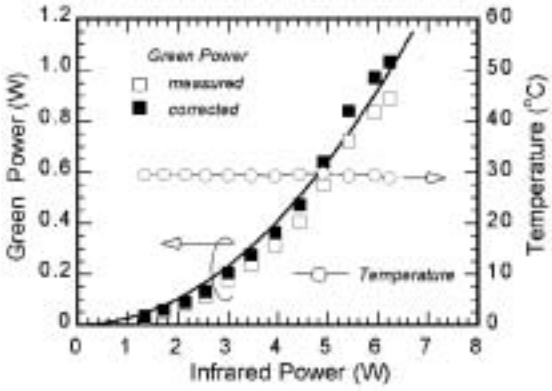

Figure 2. CW 531-nm output power (□- measured and ■- corrected with Fresnel losses) and phase matching temperature (○) *vs*. the 1063-nm incident power.

IX-B-7 Continuous-Wave High-Power Nd:YAG-$KNbO_3$ Laser at 473 nm

PAVEL, Nicolaie[1]; SHOJI, Ichiro; TAIRA, Takunori
([1]IMS and IAP-NILPRP, Romania)

[*Opt. Laser Tech.* **36**, 581 (2004)]

During the past few years much work has been done in order to obtain an efficient and simple solid-state blue laser source, this device being of interest for applications such as display technologies, production of high-density optical disk systems, high-resolution printing, or medical diagnostics. Although the blue semiconductor diode laser is expected to reach the power level necessary for these applications, the frequency-doubling of the 946-nm $^4F_{3/2} \rightarrow {}^4I_{9/2}$ transition in Nd:YAG is a practical and the most used way that leads to blue radiation at 473 nm. Various resonator configurations and nonlinear crystals could be used for frequency-doubling of a Nd:YAG laser operating at 946 nm. The first continuous-wave (CW) diode-pumped Nd:YAG laser that delivered 42-mW at 946 nm was reported by Risk and Lendth,[1)] whereas an attempt of intracavity frequency-doubling by a $LiIO_3$ nonlinear crystal yielded 100 μW of blue light. Dixon *et al.* developed the first 946-nm Nd:YAG laser intracavity frequency-doubled by a $KNbO_3$ crystal:[2)] 5-mW power at 473 nm with 2% optical-to-optical conversion efficiency with respect to the pump power, $\eta_o^{(i)}$, was obtained. A compact source of CW single-frequency radiation at 473 nm with 500 mW output power was developed, employing a diode-pumped miniature Nd:YAG ring laser as a pump source and an external semi-monolithic cavity with $KNbO_3$ crystal.[3)] The best result to date at 473 nm is an output power of 2.8 W with $\eta_o^{(i)}$ = 13.3%: the experimental set-up was a three-arms resonator and BiB_3O_6 nonlinear crystal operating at room temperature was employed for frequency-doubling.[4)]

Some disadvantages of $KNbO_3$ are a small temperature and spectral acceptance bandwidths, photorefractivity effect, and that its domain structure is easily disturbed. However, because of its high value of the nonlinear coefficient and due to its ability to be birefringently phase-matched for second harmonic generation of the 946-nm wavelength this crystal was our choice. This paper reports on our work toward scaling blue light obtained by intracavity frequency-doubling of a diode end-pumped 946-nm Nd:YAG laser, using a $KNbO_3$ nonlinear crystal.

A 1.0-at.% Nd:YAG crystal (3-mm thickness) whose surfaces were anti-reflection (AR) coated at the pumping wavelength of 809 nm and also at 946 and 1064 nm was used in experiments. To achieve efficient heat removal the Nd:YAG crystal was placed in a copper mount whose temperature was kept at 12 °C, and an indium foil was used to improve the thermal contact between the Nd:YAG and the copper heat sink. A 400-μm diameter, 0.22-NA fiber-coupled diode (HLU32 F400, LIMO Co., Germany) was used for CW pumping; the fiber was imaged into the Nd:YAG crystal in a 300-μm diameter spot. Two $KNbO_3$ crystals (Mitsui Chemicals Inc., Japan) of 1.0 and 2.0-mm thickness were cut for type I, critical-phase-matching condition (θ = 90°, ϕ = 59.2°) and placed in a copper holder whose temperature was controlled with 0.1 °C accuracy; the operation temperature was 29.2 °C. Both sides of each $KNbO_3$ were polished to parallel flat surfaces and AR coated at 473 and 946 nm.

The emission of a plane-concave resonator of 70-mm length that contains the Nd:YAG crystal, the polarizing glass plate and the $KNbO_3$ crystal was first investigated. The output mirror has 100-mm radius and it was coated as high-reflection at 946 nm and high-transmission at 473 nm. The maximum power at 473-nm for the 1.0-mm thick $KNbO_3$ crystal was 68 mW for an absorbed pump power of 3.1 W, as shown in Figure 1. The conversion of the available IR power was 10.5%. With the 2.0-mm thick $KNbO_3$ crystal the maximum blue power was 159 mW for an absorbed pump power of 3.3 W: thus $\eta_o^{(i)}$ was 2.7%, while the conversion of the IR power was determined as 21.4%. For these points of operation the transverse mode distribution was Gaussian ($M^2 < 1.05$), but a saturation of the blue power and decrease of the beam quality were obtained as the pump power was further increased.

In order to increase the blue power a V-type resonator, as shown in Figure 2, was designed. The distances M1 to M2 and M2 to M3 were 70 and 55 mm, respectively; the $KNbO_3$ nonlinear crystal was placed very close of mirror M3. Figure 3 shows the blue power versus the absorbed pump power. For the 1.0-mm thick $KNbO_3$ crystal a maximum blue power of 318 mW was obtained for an absorbed pump power of 3.8 W; the conversion efficiency of the IR power was 34.2%. An output power of 418 mW at 473 nm was recorded for the 2.0-mm thick $KNbO_3$ crystal with $\eta_o^{(i)}$ = 6.7%; the conversion of the available IR power was 50%. The 473-nm output beam was linearly polarized (> 1:10^3) and orthogonal to the 946-nm radiation. Monitoring the maximum blue output power with a powermeter resulted in ±2% power fluctuations during few hours of operation. The stability on millisecond time scale was investigated with a fast photodiode: it shows no fluctuations, indicating no blue problem. No damage of the $KNbO_3$ crystals was observed during the experiments.

For modeling of blue power, the beam distribution inside the resonator was considered independent of the

active medium refractive power induced by optical pumping, with the laser operating far of the threshold.[5),6)] Experimentally we have determined the pump coupling coefficient K_c = 0.032 W^{-1} and the loss L as ~1.5% and ~2.0% for the resonators with the 1.0 and 2.0-mm thick $KNbO_3$, respectively. The beam radius in the Nd:YAG and in $KNbO_3$ were considered independent of the absorbed power, namely 140 and 100 μm, respectively. Figure 3 also shows by continuous lines the modeling of the blue power using this model, where d_{eff} = 13 pm/V was the parameter used for fitting. The agreement between the experimental data and modeling is satisfactory, if one considers that the model assumes that the resonator parameters are optimized for each pump power, which is not the experimental case.

In conclusion, a continuous-wave diode-pumped Nd:YAG laser that operates on the 946-nm $^4F_{3/2} \rightarrow {}^4I_{9/2}$ transition and that is intracavity frequency-doubled to 473 nm using $KNbO_3$ nonlinear crystal is described. The blue maximum power was 418 mW, with 50% conversion of the available IR power, and the optical-to-optical conversion efficiency with respect to the pump power was 6.7%. To the best authors knowledge these are the highest results to date for a diode pumped Nd:YAG rod laser frequency-doubled by a $KNbO_3$ nonlinear crystal.

References

1) W. P. Risk and W. Lenth, *Opt. Lett.* **12**, 993 (1987).
2) G. J. Dixon, Z. M. Zhang, R. S. F. Chang and N. Djeu, *Opt. Lett.* **13**, 137 (1988).
3) M. Bode, I. Freitag, A. Tunnermann and H. Welling, *Opt. Lett.* **22**, 1220 (1997).
4) C. Czeranowsky, E. Heumann and G. Huber, *Opt. Lett.* **28**, 432 (2003).
5) R. G. Smith, *IEEE J. Quantum Electron.* **6**, 215 (1970).
6) A. Agnesi, A. Guandalini and G. Reali, *J. Opt. Soc. Am. B* **19**, 1078 (2002).

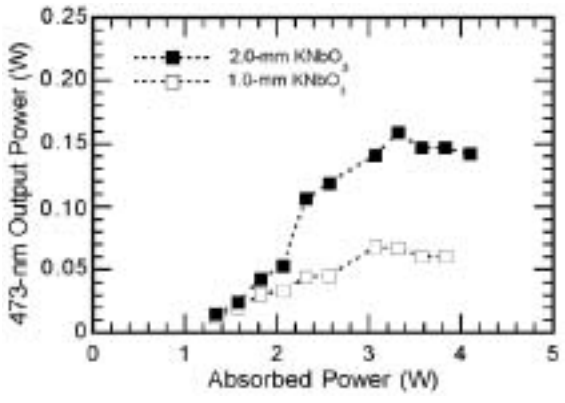

Figure 1. Blue output power *vs.* the absorbed pump power for the linear resonator.

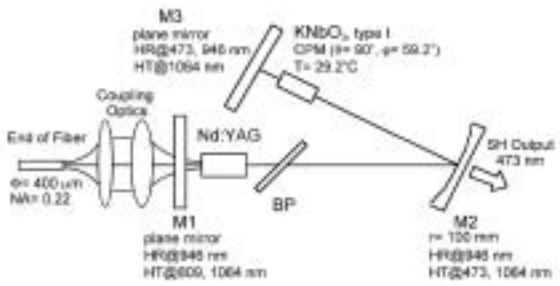

Figure 2. V-type resonator of the diode-pumped 946-nm Nd:YAG laser intracavity frequency-doubled by $KNbO_3$ crystal; BP: glass plate placed at the Brewster angle.

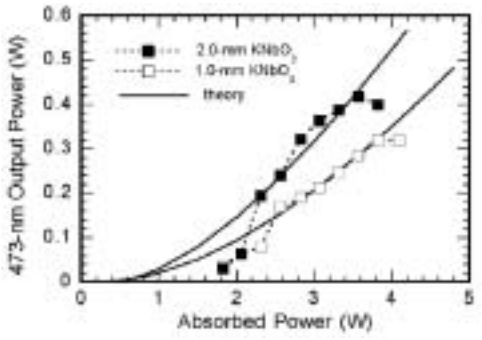

Figure 3. Blue output power *vs.* the absorbed pump power for the V-type resonator: signs for experiments and theory by the continuous lines.

IX-B-8 Room-Temperature, Continuous-Wave 1-W Green Power by Single-Pass Frequency Doubling in a Bulk Periodically Poled MgO:$LiNbO_3$ Crystal

PAVEL, Nicolaie[1]; SHOJI, Ichiro; TAIRA, Takunori; MIZUUCHI, Kiminori[2]; MORIKAWA, Akihiro; SUGITA, Tomoya[2]; YAMAMOTO, Kazuhisa[2]

([1]IMS and IAP-NILPRP, Romania; [2]Matsushita Co., Ltd., Osaka)

[*Opt. Lett.* **29**, 830 (2004)]

Due to its significant advantages of phase-matching an arbitrary wavelength and of accessing high nonlinear coefficient by using an appropriate period of polarization inversion, the second-harmonic generation (SHG) by quasi-phase-matching (QPM) interaction is an attractive method to obtain a compact and high power laser emitting into visible or ultraviolet spectral regions. Because of its simplicity, the single-pass SHG scheme is a solution to obtain continuous wave (CW) operation in blue, green, or ultraviolet ranges. This scheme requires a high nonlinear coefficient and long interaction length with noncritical phase matching: these conditions are well fulfilled by the periodically poled $LiNbO_3$ (PPLN) crystal. It is known, however, that PPLN has significant problems for visible light radiation, such as green- or blue-induced infrared absorption and optical damage. Although phase matching at high temperature of 200 °C[1)] or 140 °C[2)] was used, power instabilities and thermal lens effects could not be completely suppressed.

To overcome these problems, the use of periodically poled MgO:$LiNbO_3$ (PPMgLN) was proposed:[3] this crystal presents larger nonlinear susceptibilities, higher resistance against photorefractive damage and shorter wavelength transparency compared with PPLN. CW blue power of 17.3 mW at 426 nm was demonstrated from a PPMgLN waveguide that was single-pass pumped by a AlGaAs diode laser.[4] A novel high-voltage multi-pulse poling technique that suppress the penetration of poled region and produces uniform PPMgLN with domain period (Λ) as short as 1.4 μm was developed by our group: ultraviolet light at 341.5 nm with a normalized conversion efficiency of 5.4%/W was thus demonstrated.[5] In this letter we report high-power CW frequency-doubling at room temperature in a first-order PPMgLN of Λ = 6.95-μm fabricated by this technique and that was single-pass pumped with a Nd:$GdVO_4$ laser operating at one micron wavelength.

The experimental set-up is shown schematically in Figure 1. Taking into account the high thermal conductivity of Nd:$GdVO_4$ and the fact that the output beam is polarized, a diode-end pumped Nd:$GdVO_4$ laser (Z-type resonator) was build as a pump source: the laser delivers 6.8 W with 45% optical-to-optical efficiency, in a beam with M^2 factor of 1.15; the slope efficiency was 57%. The output beam depolarization ratio was 1.2% and the power fluctuation during few hours of operation was ±1.1%. The laser spectrum, which was investigated by a spectrum analyzer (Q8384 Advantest Co., Japan) with 0.01-nm resolution, was centered at 1062.9 nm and presented four peaks separated by 0.08 nm, each peak with FWHM of ~0.01 nm; the spectrum width was ~0.24 nm.

The fabrication process of PPMgLN with Λ = 6.95-μm and long interaction length was as follows: To obtain a uniform PPMgLN structure over large areas, local penetration of polarization-inverted regions was suppressed by using a thick crystal and the multi-pulse application method.[6] A Z-cut 5-mol% MgO doped LN crystals of 2-mm thickness were used. First, a 100-nm thick Ta film was sputtered on the +Z and –Z faces of the crystals. Next, the patterned electrodes were covered with a 200-nm thick sputtered SiO_2 film. The applied voltage and pulse width were 10 kV and 1 ms, respectively. During the poling process, to lower the coercive field, the samples were heated at ~ 140 °C. After poling the substrate was etched in a 1:2 HNO_3+HF solution at 60 °C for several minutes to reveal the polarization-inverted region on both surfaces of the crystal. The cross sections were examined by cutting samples along Y-faces, polishing and etching. It was found that the structure has 50% duty cycle from the +Z surface to a depth of ~300 μm and uniform periodicity was maintained from the surface to ~800-μm depth; however, the polarization-inverted regions were not realized near the –Z face.

For SHG experiments PPMgLN crystals of 10- and 25-mm length were cut from the poled samples and the end-faces were optically polished and antireflection (AR) coated by SiO_2 monolayer for the 1063-nm wavelength; the SiO_2 coating has no AR effect at 531 nm. The PPMgLN were placed on an aluminum plate whose temperature was controlled within 0.1 °C accuracy using a thermoelectric cooler. A dichroic mirror M, coated as high-reflectivity for 1063 nm and as high-transmission for 531 nm, was used to reflect the fundamental radiation left after PPMgLN.

A maximum CW green power of 0.89 W was measured for the 10-mm-long PPMgLN for an incident infrared power of 6.23 W. If the Fresnel loss (~14%) on the output surface of PPMgLN is considered the maximum internal green-light power results as 1.03 W, corresponding to a conversion efficiency of 16.5%. Figure 2a shows the internal green power and conversion efficiency versus the 1063-nm input power in PPMgLN. The effective nonlinear coefficient was determined as 14 pm/V; thus, the normalized conversion efficiency including the Fresnel loss by reflection was 3.0%/W. For the 25-mm long PPMgLN crystal a maximum green power of 1.18 W was measured. When the Fresnel loss is considered (Figure 2b) the internal power and conversion efficiency were 1.38 W and 19.6%, respectively, while the normalized conversion efficiency was ~3.3%/W; the continuous line of Figure 2b shows the expected results with this value.

The phase matching temperature was 29.5 °C, stable within ±0.3 °C on the entire pumping range. The experimental data for the acceptance bandwidth ΔT was 3.9 °C, while the theoretical value obtained by taking into account the Sellmeier equations for LN crystal[7] resulted as 3.4 °C; good agreement could be observed. During few hours of operation output power instabilities or variations of the green beam pattern that could be caused by thermal lens effects or optical damage of PPMgLN were not observed. Then, the strong resistance against photorefractive damage of MgO:$LiNbO_3$ enables achieving this green power level and highly efficient SHG efficiency in a CW single-pass pumping scheme.

In conclusion, CW power of 1.18 W at 531 nm with 16.8% power conversion efficiency was obtained from a 25-mm-long uncoated bulk PPMgLN in a single-pass frequency doubling scheme using a Nd:GdVO4 laser as pumping source; the PPMgLN internal power of and conversion efficiency were 1.38 W and 19.6%, respectively. To the authors best knowledge this is the highest power ever reported by quasi-phase matching at room temperature. The present result supports the prospect of obtaining compact and high power visible source based on bulk periodically poled MgO:$LiNbO_3$.

References

1) G. D. Miller, R. G. Batchko, W. M. Tulloch, D. R. Weise, M. M. Fejer and R. L. Byer, *Opt. Lett.* **22**, 1834 (1997).
2) G. W. Ross, M. Pollnau, P. G. R. Smith, W. A. Clarkson, P. E. Britton and D. C. Hanna, *Opt. Lett.* **23**, 171 (1998).
3) K. Mizuuchi, K. Yamamoto and M. Kato, *Electron. Lett.* **32**, 2091 (1996).
4) T. Sugita, K. Mizuuchi, Y. Kitaoka and K. Yamamoto, *Opt. Lett.* **24**, 1590 (1999).
5) K. Mizuuchi, A. Morikawa, T. Sugita and K. Yamamoto, *Jpn. J. Appl. Phys.* **42**, L90 (2003).
6) T. Sugita, K. Mizuuchi, Y. Kitaoka and K. Yamamoto, *Jpn. J. Appl. Phys.* **40**, 1751 (2001).
7) G. J. Edwards and M. Lawrence, *Opt. Quantum Electron.* **16**, 373 (1984).

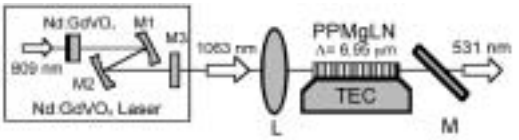

Figure 1. The experimental set-up used for SHG generation. L: focusing lens, TEC: thermoelectric cooler, M1, M2, M3, M: mirrors.

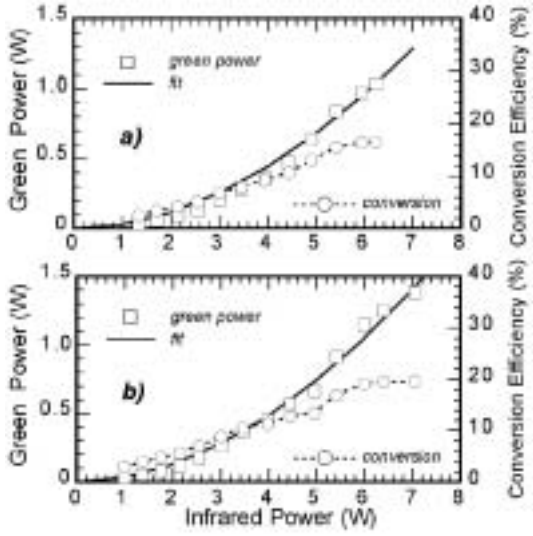

Figure 2. Internal cw 531-nm output power and internal conversion efficiency versus the 1063-nm incident power for a) 10-mm and b) 25-mm long PPMgLN. Continuous lines shows the modeling with a quadratic dependence.